Non-thermal plasma: A fast and efficient template removal approach allowing for new insights to the SBA-15 structure

Thibaud Aumond, Ludovic Pinard, Catherine Batiot-Dupeyrat, Alexander Sachse

Non-Thermal Plasma: A Fast and Efficient Template Removal Approach Allowing for New Insights to the SBA-15 Structure

Thibaud Aumond, Ludovic Pinard, Catherine Batiot-Dupeyrat, Alexander Sachse*

Université de Poitiers, Institut de Chimie des Milieux et Matériaux de Poitiers (IC2MP) - UMR 7285 CNRS, UFR SFA, Bât. B27, 4 rue Michel Brunet, TSA 51106, 86073 Poitiers Cedex 9 – France

*corresponding author: alexander.sachse@univ-poitiers.fr

Abstract

Non-thermal plasma has revealed as fast and efficient strategy for the complete elimination of template molecules from SBA-15 materials. Through comparing the textural properties of a set of SBA-15 materials obtained by classical calcination and non-thermal plasma treatment new insights to the SBA-15 structure could be revealed. As such, a third type of microporosity could be disclosed by the use of non-thermal plasma for SBA-15 synthesized at 60 °C. Additionally, starting from a synthesis temperature of 100 °C, template elimination through non-thermal plasma allows for preserving native textural properties of as-synthesized SBA-15. The developed alternative treatment combines the advantages of improved textural properties and higher silanol density, hence making the strategy very promising for superior applications of SBA-15 materials.

Keywords: SBA-15, non-thermal plasma, template removal, surfactants, textural properties, porosity.

1. Introduction

The development of ordered mesoporous materials has been in the focus of materials research for almost three decades now. One of the most fascinating and widely described members of the ordered mesopores silica family featuring hexagonally ordered pores is SBA-15.[1,2] Despite the huge amount of reports dealing with potential applications of SBA-15,[3] some open questions as far as the exact textural properties of SBA-15 are concerned still prevail. Partially, this can be explained by the fact that the structure of SBA-15 is critically affected by the synthesis temperature. It has indeed been described that low synthesis temperatures favor the development of micropores next to hexagonally ordered mesoporosity, whilst high temperatures lead to materials that are purely mesoporous in nature. The presence of microporosity in some SBA-15 materials was firstly indicated by Stucky and co-workers based on nitrogen adsorption.[4] Soon after, Ryoo *et al*.[5] described the presence of secondary porosity present in the pore walls through the grafting of organosilanes of different bulkiness on the surface of SBA-15. Impéror-Clerc *et al*.[6] depicted the SBA-15 structure as featuring a microporous corona around the larger mesopores through careful modeling of the achieved XRD intensities. Galarneau *et al.*[7] pointed out the difficulty to describe the porous structure of SBA-15 based on the presence of a very wide size distribution of small pores ranging from the microporous to the smaller mesoporous range. It was indeed evidenced that micropores are of a wide size distribution and span over even the small mesopore range with sizes smaller than 3.4 nm.[8] Silvestre-Albero and co-workers, preformed *n*-nonane preadsorption followed by nitrogen physisorption on SBA-15 materials and evidenced merely a very little fraction of micropores.[9] Careful observation of inverse platinum replica of SBA-15 samples revealed that some of these small mesopores interconnect the ordered larger mesoporosity.[10]

Further misconstruction of the SBA-15 structure is often related to the characterization of SBA-15 upon the removal of the template. Indeed, one of the key steps in the synthesis of the SBA-15 materials is the elimination of the organic surfactant. The most widely used technique for this purpose is calcination in air at temperatures comprised between 500 and 600 °C for several hours. Calcination at these temperatures is extremely efficient as it allows to remove the integrity of the organic surfactant.[11,12] The major drawback of calcination is the coherent lattice shrinkage and which further

importantly reduces or even leads to complete destruction of microporosity.[13] Yet, important conclusions on the texture of SBA-15 materials have been inferred for materials calcined at elevated temperatures.[10]

With the aim to develop milder template removal strategies from as-synthesized SBA-15 materials a series of alternative approaches has been put forward. The liquid extractions with solvents[14] or supercritical fluid extraction with CO_2[15] are appealing strategies as templates can be recovered and hence recycled, yet templating removal efficiency is limited to 60-80% even after various extraction cycles, which implies the necessity of further treatments. Besides calcination, oxidative treatments based on the digestion with H_2O_2,[16-19] and plasma assisted template degradation have been reported for the elimination of Pluronic templated silicas. Saito and co-workers developed a solution plasma process in which active species based on O, H and OH *in situ* develop from the aqueous solution.[20] The efficiency of the process has been described to critically depend on the pH and that the treatment efficiency is highest in alkaline and acidic media. Though, it has been reported that templates can be fully removed within 15 min through this process it remains disputable as textured silicas are highly sensitive to exposures to alkaline environments.[21] Moreover, template molecules from SBA-15 were completely removed using glow discharge plasma (GDP).[22] The inconvenience of GDP is the long exposure time required in order to remove fully the template (2 h). Finally a stepwise template removal process was developed by Schüth and co-workers in which the template ethers in the large mesopores are first cleaved using concentrated sulfuric acid solutions followed by a thermal calcination at 200 °C, which allows to remove the integrity of the template from micropores.[23,24] These latter approaches state to entirely remove the template from SBA-15, yet textural characterizations were not carried out with sufficient depth to allow for the carful observation of textural features.

Non-thermal plasma (NTP) has revealed extremely efficient to degrade organic molecules by a highly oxidizing environment at room temperature. Indeed, NTP has allowed for eliminating structure directing agents form as-synthesized zeolites and MCM-41.[25-28] Yet, rather long exposure times (> 2 h) have been reported for full elimination of templates. Recently the coke elimination from spent zeolite catalysts through the use of NTP in O_2/He mixtures was described. Helium revealed as significantly better energy carrier and allowed hence for reducing plasma treatment times considerably.[29-31]

The scope of this contribution is to investigated NTP using O_2/He mixtures as alternative template removal strategy, with the aim to preserve textural properties of the as-synthesized SBA-15 materials and hence to achieve new insights on its structure. To the best of our knowledge this is the first report that describes the use of NTP for Pluronic template removal in SBA-15.

2. Materials and Methods

2.1 Materials

HCl (37%, Fisher Scientific), NH_4OH (30%, Aldrich), tetraethylorthosilicate (TEOS, Merck) and Pluronic P123 (Sigma-Aldrich) were purchased and used as received.

2.2 Synthesis of SBA-15

2.2.1 As-synthesized SBA-15

In a 250 mL beaker 1 g of Pluronic P123 was dissolved in 15 mL of a 2 M aqueous HCl solution under constant agitation at 35 °C for 1 hour. 2.1 g of TEOS are subsequently drop-wise added to the former solution at under agitation. The molar composition of the mixture was 1P123:11.7TEOS:34.8HCl:966.1H_2O. After complete addition of the silica source the mixture was aged at 35 °C during 24 h and then subsequently heated to the target synthesis temperature (60, 80, 100 or 130 °C) for 24 h in a sealed Teflon autoclave. After cooling to RT, the synthesis mixture was centrifuged, and the residual solid washed three times with distilled water and dried at 60 °C during 72 h. Samples were named SBA15-X in which X stands for the synthesis temperature, *i.e.* 60, 80, 100 and 130.

2.2.2 Template removal through calcination

Calcination was carried out in a muffle furnace of a total volume of 25 L under air. 100 mg of dry samples were finely dispersed on a ceramic support and placed at the center of the furnace. Heating rate was 2 °C/min until target temperature, which was kept constant for 4 h, before cooling to RT. Calcination temperatures of 300, 400, 550, 750 and 850 °C were used. Samples were named SBA15-X-Y, in which Y stands for the calcination temperature.

2.2.3 Template removal through NTP

A quartz reactor of the dimensions 10 x 120 mm equip with a gas inlet and outlet and featuring an inner stainless steel electrode (3 mm) and an outer copper electrode (20 mm) wrapped around the reactor was used (**Scheme S1**). The gap of the internal electrode and the reactor walls was 2.5 mm. The two electrodes were connected to a bipolar pulse generator A2E Technologies-Electronic. Two consecutive pulses U_+ and U_- were applied to one electrode and then to the second one. The deposited power (P) was calculated from the time averaged product of discharge voltage and current. 200 mg of the as-synthesized SBA-15 were placed on a grid in the reactor. A 80/20 helium/oxygen mixture was used with a flow rate of 100 mL min^{-1}. The frequency was set to 2000 Hz and a voltage of 8 kV was applied for 15 minutes (7 W).

2.6 Characterization

2.6.1 Physisorption isotherms

Nitrogen physisorption isotherms were recorded at -196 °C using a Micromeritics 3FLEX instrument. Before analysis, all samples were outgassed under secondary vacuum for 12 h at RT. The nitrogen adsorption and desorption isotherms are represented by plotting the adsorbed volume as function of the relative pressure. The *t*-plots were achieved using the reference isotherm for the synthesized non porous silica material described in the supplementary information (**Table S1**). In contrast to macroscopic approaches, DFT allows to obtain accurate pore size analysis even for narrow micro- and mesopores.[32] DFT pore size distributions were realized with the Micromeritics software taking into consideration cylindrical pore shape. The applicability of the model was tested for a mechanical mixture containing various degrees of meso- and microporosity as described in the supplementary information (**Figure S1**). Total pore volume (V_{tot}) was determined at the relative pressure of 0.95 from nitrogen adsorption isotherms at -196 °C.

2.6.2 X-ray diffraction

Powder diffractograms were collected using a PANalytical Empyrean X-ray diffractometer using CuKα radiation (1.54059 Å), for the 2θ range from 0.5 to 5°. The scan speed was fixed at 0.008° min^{-1}. Lattice parameters (a_0) were calculated using following relations for a hexagonal system:

$$a_0 = 2\frac{d_{(100)}}{\sqrt{3}}$$

$$a_0 = 2d_{(110)}$$

$$a_0 = 4\frac{d_{(200)}}{\sqrt{3}}$$

where $d_{(100)}$, $d_{(110)}$ and $d_{(200)}$ correspond to the distance of the (100), (110) and (200) planes, respectively.

2.6.3 Transmission electron microscopy

Transmission electronic microscopy (TEM) was performed over selected samples using a JEOL 2100 instrument (operating at 200 kV with a LaB_6 source and equipped with a Gatan Ultra scan camera). Lattice parameters were calculated using the Gatan software.

2.6.4 Thermo gravimetric analysis (TGA) and elemental analysis

TGA was performed on a Q600 TA Instruments. 10 mg of the sample were weighted in the crucible and heated to 900 ° C with a ramp of 10 ° C min^{-1} in air flow (50 mL min^{-1}). The percentage of organic was achieved from the mass loss in the temperature range from 100-400 °C. The amount of water formed from silanol condensation was inferred from mass loss in the temperature range from 400-900 °C.

Elemental analysis was carried out on a Flash EA 1112 / Flash 2000 Thermo in order to quantify the amount of carbon present on samples.

3. Results and discussion

3.1 Template removal from SBA-15 materials through calcination in air

A set of SBA-15 materials were prepared at 60, 80, 100 and 130 °C. The as-synthesized materials were calcined at 550 °C in air. For all of the calcined samples type IV isotherms were observed in nitrogen physisorption at -196 °C (**Figure 1a**), which are characteristic for samples in which capillary condensation occurs. The synthesis at the lowest temperature (60 °C) yields the SBA-15 material with the lowest total pore volume and the smallest size of hexagonal ordered mesopores, which is centered at 7.0 nm. With increasing synthesis temperature the size of these mesopores increases and is of 8.8, 9.5 and 12.8 nm for synthesis temperatures of 80, 100 and 130 °C, respectively (**Figure 1c**).

As far as microporosity is concerned both synthesis at 60 and 80 °C present a comparable pore size distribution, featuring maxima centered at 1.1 and 2.0 nm (**Figure 1b**). The sample synthesized at 100 °C shows very little microporosity (0.01 cm^3 g^{-1}) and features a pore size distribution centered in the very small mesoporous range (2.2 nm). When synthesis is carried out at 130 °C, the size distribution of these small mesopores shifts to 3 nm. It is furthermore worth to mention that for all of the samples some wider mesopores with large size distribution between 3 and 7 nm can be observed. The obtained results compare well to what has previously been reported in the literature with the exception that smaller mesopores are observed for all samples even those achieved at low synthesis temperature (60 °C).

It is interesting to note that the lattice parameter is similar for all of the as-synthesized material (and is comprised within 11.2 and 11.8 nm (**Table S2**). The effect of calcination on the materials leads to a drastic reduction of the lattice parameter (**Table 1**). The sample synthesized at 130 °C shows the smallest reduction of the lattice parameter upon calcination, which can be ascribed to the absence of

microporosity in this sample. Lattice shrinkage is hence importantly related to the amount of surfactant enclosed within the pore walls. Indeed, though total porous volume is maximal for SBA15-130-550 it features the lowest amount of surfactant in the as-synthesized material (**Table S3**).

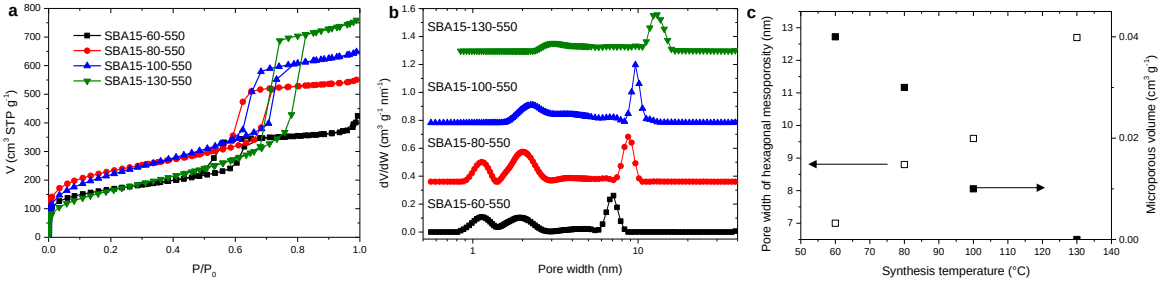

Figure 1. Nitrogen adsorption and desorption isotherms at -196 °C (a) and DFT pore size distributions (b) for SBA15-60 (black), -80 (red), -100 (blue), and -130 (green) calcined at 550 °C. c) Evolution of the pore width of hexagonal mesoporosity and microporous volume as a function of synthesis temperature. Plots are shifted on the y axis for DFT pore size distributions.

As indicated by Galarneau *et al.*[7] the use of standard *t*-plot is critical for deducing microporous volume of SBA-15 material. Indeed, through applying the Harkins-Jura approach a constant multilayer adsorption is observed prior to capillary condensation (**Figure S3a**). To circumvent the limitations of the Harkins-Jura plot, a purely non-porous silica was synthesized in order to achieve a suitable reference isotherm to construct the *t*-plot (**Table S1**). Using the designed *t*-plot the deviation from the linearity from multilayer adsorption is well observed before capillary condensation, which can readily be ascribed to the fraction of smaller mesopores that cannot to be identified through the standard *t*-plot procedure. Hence, applying values of the *t*-plot in the fitting range of 2 and 3 nm allows to assess the microporous volume, which compares well to the cumulative pore volume achieved by the DFT model. Microporous volume decreases linearly as a function of the synthesis temperature and is null for the sample achieved at 130 °C (**Figure 1c**).

One of the key steps in the synthesis of SBA-15 is the elimination of the template from the as-synthesized materials, which allows to develop the porosity. Though the degradation of the Pluoronic template initiates at 160 °C, its complete elimination requires calcination temperatures of at least 400 °C (**Figure S4, Table S4**). Hence, in the scientific literature SBA-15 materials are usually

calcined at temperatures between 400 and 600 °C in order to totally eliminate the template.[6-8,10,16] Yet, calcination temperature has a major impact on the textural properties of the SBA-15 materials.

For the sample SBA15-60; though calcined at 300 °C does not permit to remove the integrity of the surfactant (> 2% of surfactant can be evidenced by elemental analysis, **Table S4**); it is the sample that features the highest porous volume (**Figure 2**). Increasing the synthesis temperature importantly reduces both meso- and microporous volume. As a matter of fact microporosity drops linearly from 0.075 to 0.001 cm^3 g^{-1} for calcination temperatures of 300 to 750 °C, respectively (**Figure 2c**). Calcination temperatures of above 750 °C lead to complete deterioration of microporosity, yet a minor fraction of intermediate mesopores (3-5 nm) persist (**Figure 2b**).

The decrease of microporosity is concomitant with lattice shrinkage. The size of the hexagonal mesoporosity decrease from 7.65 to 5.90 nm for SBA15-60 material calcined at 300 and 850 °C, respectively. This finding was confirmed from XRD, as lattice parameters decrease essentially over 2.5 nm from the lowest to the highest calcination temperature (**Figure S2, Table 1**).

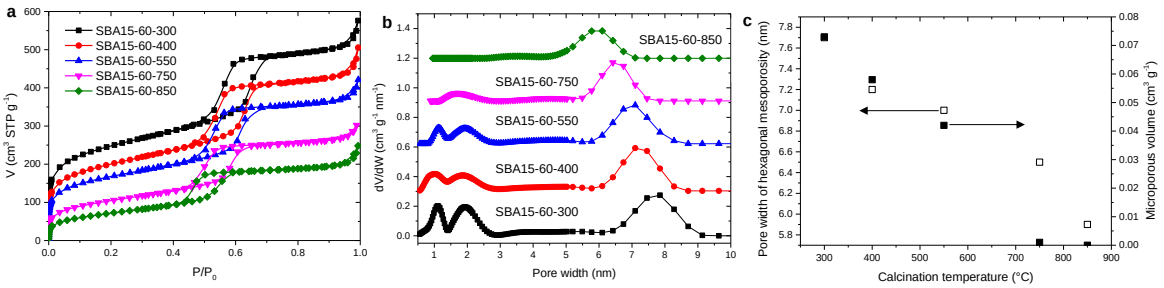

Figure 2. Nitrogen adsorption and desorption isotherms at -196 °C (a) and DFT pore size distributions (b) of SBA-15-60 calcined at different temperatures. c) Evolution of pore width of hexagonal mesoporosity and of microporous volume as a function of the calcination temperature. Plots are shifted on the y axis for DFT pore size distributions.

Table 1. Textural parameters for calcined SBA-15 materials.

Sample	a_0 (nm)	V_{tot} (cm^3 g^{-1})	V_{micro} (cm^3 g^{-1})	Pore width[a] (nm)
SBA15-60-300	10.1	0.73	0.074	7.7
SBA15-60-400	9.9	0.62	0.058	7.2
SBA15-60-550	9.7	0.53	0.042	7.0
SBA15-60-750	8.9	0.37	0.001	6.5
SBA15-60-850	8.5	0.28	0	5.9
SBA15-80-550	10.4	0.83	0.035	8.8
SBA15-100-550	10.5	0.97	0.012	9.6

SBA15-130-550	11.2	1.12	0	12.7

[a]of hexagonal ordered mesoporosity.

Calcination in air is doubtlessly a rather simple and cost efficient process, which allows for the complete removal of the surfactant form as-synthesized SBA-15 materials at a certain temperature (>400 °C). Calcination yet importantly affects the texture of the materials as microporosity is doomed to a certain extent, impacting wall thickness and pore size distribution. In order to thoroughly characterize textural properties of SBA-15 calcination rather seems an inconvenient template removal strategy.

3.2 Template removal from SBA-15 materials through NTP

Due to the previously stated limitation of thermal treatments for the removal of the template from SBA-15 materials we investigated NTP as alternative template removal strategy, with the aim to preserve textural properties of the as-synthesized samples and hence to achieve new insights on their structure.

The as-synthesized sample that presents the highest amount of potential microporosity (SBA15-60) was treated with NTP at a deposited power of 7 W (2000 Hz, 8 kV) during 15 min. The obtained nitrogen physisorption isotherm compares well to the one achieved for the calcined sample at 300 °C (**Figure 3a**), yet SBA15-NTP features a higher total pore volume (0.83 cm^3 g^{-1}) and the absence of any organic residue (as inferred from elemental analysis). Important differences are further observed when comparing the DFT pore size distribution. The most striking feature of the NTP treatment is that it allows for developing ultramicroporosity with a pore width centered at 0.7 nm (**Figure 3b**). The further porosities compare to what was revealed for the calcined samples at 300 and even 550 °C. As far as the hexagonal structured mesoporosity is concerned it is slightly larger for the NTP treated sample and is centered at 8.01 nm. Both, development of ultramicropores and larger hexagonal mesoporosity suggest a less pronounced shrinkage of the lattice. Indeed, from XRD a larger lattice parameter was calculated for SBA15-NTP, which amounts to 10.3 nm (**Table 2, Figure S5**).

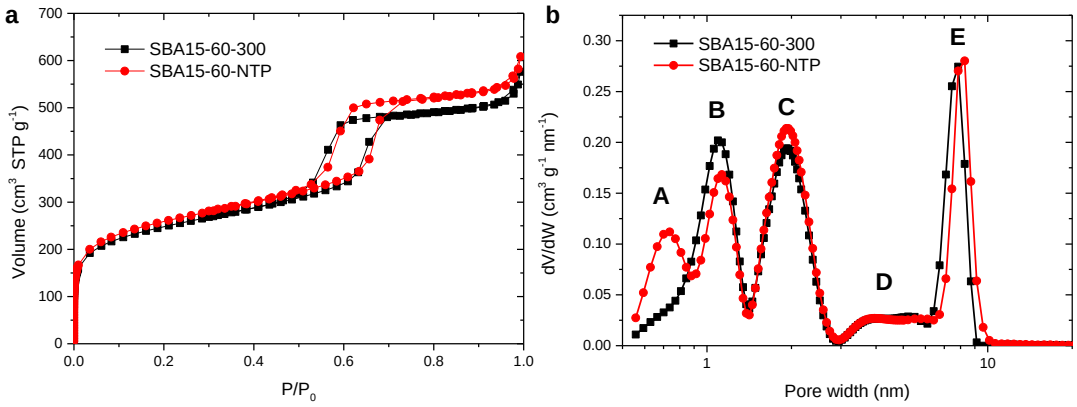

Figure 3. Comparison of nitrogen adsorption and desorption isotherms at -196 °C (a) and DFT pore size distributions (b) of SBA15-60 calcined at 300 °C (black) and treated with NTP (red).

NTP hence allows for preparing samples that are less affected by lattice shrinkage. Indeed, for the SBA15-100 identical lattice parameter is achieved through NTP as for the as-synthesized sample (**Table S2**), which suggests that almost native properties of the SBA-15 materials can be preserved. For the sake of comparison the various porous features of SBA-15 materials were classified in five groups and attributed with the letters A-E as indicated in Figure 3b and in which A type pores correspond to ultramicropores (0.6-0.8 nm), B to micropores (0.9-1.3 nm), C to supramicropores (1.4-2.4 nm), D to small mesopores (3.2-5.0 nm) and E to hexagonally ordered mesopores (6.0-13.0 nm). The use of NTP allows for preserving the smallest type of porosity of SBA-15 based samples that is lost through calcinations at 550 °C (**Figure 4**). As such, for SBA15-100 the use of NTP allows to achieve samples in which micropores of type B are present whilst for the calcined sample the smallest porosity is of type C (**Figure 4 and S6**). Likewise for SBA15-130, NTP treatment allows for achieving a material in which C-type porosity is present, yet for the calcined sample the smallest observed porosity is of type D. Moreover, the NTP treatments lead to materials with higher total pore volume for all of the samples (**Figure S7**).

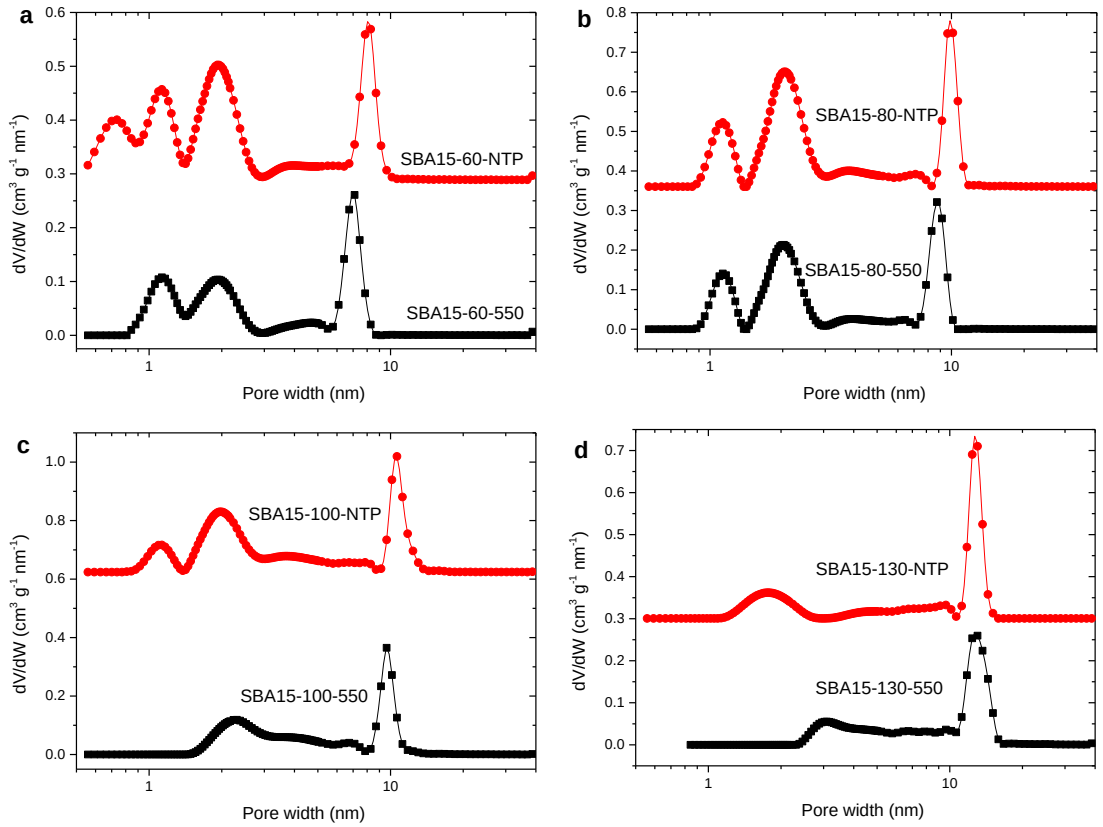

Figure 4. DFT pore size distributions for SBA15-60 (a), -80 (b), -100 (c) and -130 (d) for calcined at 550 °C (black) and NTP treated (red) samples. Plots of NTP treated samples are shifted on the y axis.

Table 2. Textural properties of SBA-15 materials treated with NTP.

Sample	a_0 (nm)	V_{tot} (cm^3 g^{-1})	V_{micro} (cm^3 g^{-1})	Pore width[a] (nm)
SBA15-60-NTP	10.3	0.84	0.078	8.0
SBA15-80- NTP	10.9	1.11	0.042	9.9
SBA15-100- NTP	10.7	1.21	0.032	10.5
SBA15-130- NTP	11.2	1.15	0	12.9

[a]of hexagonal ordered mesoporosity.

In order to gather further insights on the structure of samples, their texture was investigated through transmission electron microscopy. Despite the important amount of microporosity and small mesoporosity present in SBA15-80 merely the hexagonal ordered mesopores were inferred, which indicates that the various porous levels are integrated homogeneously within the pore walls formed by the hexagonal ordered pores (**Figure 5**). As expected synthesis at 80 °C leads to the observation of smaller mesopores and thicker pore walls compared to the synthesis at 130 °C. For both calcination at 550 °C and NTP treatment the lattice parameters were calculated from the TEM images (**Table S5,**

Figure S7). Though these revel to be slightly smaller than those calculated from the diffractograms the same tendency between calcined and NTP treated samples was inferred. It is to note that obtaining smaller lattice parameters from TEM compared to XRD has been previously reported.[33]

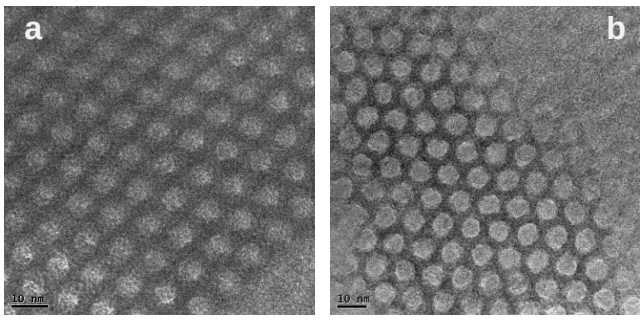

Figure 5. TEM images of SBA15-80-NTP (a) and SBA15-130-NTP (b).

As expected, by applying NTP for removing the template from SBA-15 leads to materials that feature a higher density of surface silanol groups. Indeed the amount of water formed by silanol condensation allows to indirect assessing the amount of silanol groups present on the surface of the samples (**Figure S8**). For calcined samples a significantly lower percentage of silanol condensation was observed compared to the NTP treatment independently of the synthesis temperature (**Table S6**). Important reduction of silanol groups is inevitable during calcination,[34] whilst in the present study the NTP process operating at room temperature permits to preserve these functions.

The exact reaction mechanism of the template removal under NTP is difficult to establish as numerous active species are generated under such conditions, including the positive ion O_2^+, the negative ions O^-, O_2^- and further O_3.[35] The direct oxidation of the template molecules is expected to occur, which is inferred from the composition of the exhaust gas (mainly CO and CO_2 associated with H_2O). The involvement of hydroxyl radicals $HO^\bullet$ can further be assumed, which may be formed from water dissociation[36] and considered a powerful oxidizing agent.[37]

3.3 Liberation of porosity through NTP

With the aim to achieve further insights to the template degradation mechanism the sample SBA15-100 was characterized after various durations of exposure to NTP. From the nitrogen physisorption

data was inferred that the porosity develops essentially within the first 10 minutes of treatment (**Figure 6**). After 15 minutes of treatment the textural properties remain constant (**Table 3 Figure S9**). The material achieved after 1 min of treatment merely leads to the liberation of 15% of the total porosity, which relates exclusively to the ordered hexagonal pores (**Figure 6b and c**). Within 5 minutes of NTP small mesopores and hexagonal mesoporosity develops. After 10 minutes of treatment microporosity further develops. Thereafter, textural features remain almost constant. An initial volume liberation rate of 0.176 cm^3 g^{-1} min^{-1} was found. It is further interesting to observe that the pore size distribution of the hexagonal ordered mesoporosity evolves throughout the treatment and is 8.8 nm after 1 minute and develops rapidly to the final pore size (10.5 nm) within 10 minutes of treatment (**Table 3**). The absence of hysteresis due to cavitation in all of the isotherms indicates that the surfactant is homogenously removed from the pores and that no pore plugging occurs during template elimination by residual surfactant-fragments (**Figure 6**).

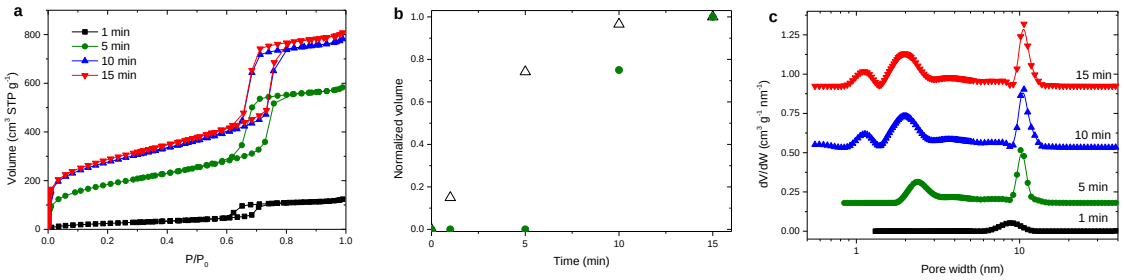

Figure 6. a) Nitrogen adsorption and desorption isotherms at -196 °C of SBA-15-100 treated with NTP for various durations. b) Evolution of the normalized mesoporous volume (void symbol) and microporous volume (full symbol) for SBA-15-100. C) DFT pore size distribution from N_2 physisorption isotherms at -196 °C.

Table 3. Textural parameters of SBA-15-100 treated with NTP at different durations.

Treatment time (min)	V_{tot} (cm^3 g^{-1})	V_{micro} (cm^3 g^{-1})	Pore width[a] (nm)
1	0.18	0	8.8
5	0.87	0	10.3
10	1.17	0.03	10.5
15	1.21	0.04	10.5
60	1.21	0.04	10.5
240	1.21	0.04	10.5

[a]of hexagonal ordered mesoporosity.

Taking all of the achieved evidence from NTP treated SBA-15 samples together a full picture on the textural properties of the materials can be drawn and is summarized in scheme 1. Here all of the levels of porosity are depicted for the SBA-15 materials achieved at different temperatures. It is well known that micropores in low-temperature SBA-15 result from intermicellar interactions.[5] Through increasing the synthesis temperature these diminish to the expense of intramicellar interactions. The smallest level of porosity (*i.e*. the ultramicropores revealed in this study) may well result from the embedding of single PEO strands of the surfactant within pore walls. The higher levels of porosities result accordingly from multiple PEO strand interactions that are favored as synthesis temperature increases.

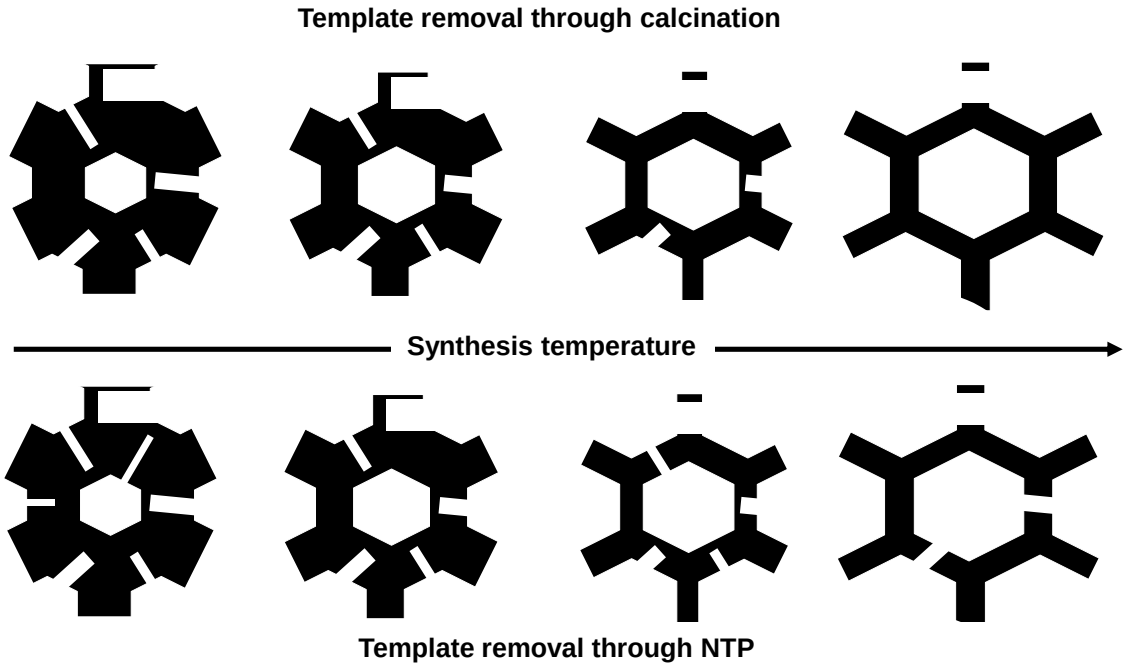

Scheme 1. Schematic representation of porosities in SBA-15 materials achieved through calcination and NTP.

4. Conclusion

NTP has revealed as extremely powerful strategy in the quest of achieving new insights of the structure of SBA-15 materials. Whilst calcination at elevated temperatures (> 400 °C) is the technique of choice for the removal of structure directing agents from inorganic materials, their final textural properties are importantly impacted by this procedure. The use of NTP allows for preserving almost

native properties of the as-synthetized SBA-15 materials. As such, the use of NTP has allowed for the first observation of ultramicroporosity within SBA-15 materials synthesized at 60 °C. Samples treated through NTP are less affected by lattice shrinkage. NTP hence permits for achieving SBA-15 materials with increased textural properties that furthermore feature a higher degree of surface silanol groups, which hence are susceptible to improved surface functionalization. This could lead to the development of SBA-15 based adsorbents or catalysts with superior capacities and activity. NTP is a very promising strategy for the fast and efficient removal of organic species from inorganic materials and is especially suited for materials which textural properties are sensitive to elevated temperatures.

Supporting Information

Description of the NTP set-up, validity of the DFT model, construction of the *t*-plot, additional pore size distributions, XRD spectra, TGA curves and additional TEM images are available as supporting information.

ACKNOWLEDGMENTS

The authors acknowledge financial support from the European Union (ERDF) and "Région Nouvelle Aquitaine".

REFERENCES

1. D. Y. Zhao, J. L. Feng, Q. S. Huo, N. Melosh, G. H. Fredrickson, B. F. Chmelka, G. D. Stucky, Triblock Copolymer Syntheses of Mesoporous Silica with Periodic 50 to 300 Angstrom Pores, *Science* **1998**, *279*, 548-552.
2. Y. Wan, D. Zhao, On the Controllable Soft-Templating Approach to Mesoporous Silicates, *Chem. Rev.* **2009**, *109*, 1613-1629.
3. P. Munnik, P. E. de Jongh, K. P. de Jong, Recent Developments in the Synthesis of Supported Catalysts, *Chem. Rev*. **2015**, *115*, 6687−6718.

4. W. W. Lukens, P. Schmidt-Winkel, D. Zhao, J. Feng, G. D. Stucky, Evaluating pore sizes in mesoporous materials: A simplified standard adsorption method and a simplified Broekhoff-de Boer Method, *Langmuir* **1999**, *15*, 5403-5409.
5. R. Ryoo, C. H. Ko, M. Kruk, V. Antochshuk, M. Jaroniec, Block-Copolymer-Templated Ordered Mesoporous Silica: Array of Uniform Mesopores or Mesopore−Micropore Network?, *J. Phys. Chem. B* **2000**, *104*, 11465-11471.
6. M. Impéror-Clerc, P. Davidson, A. Davidson, Existence of a Microporous Corona around the Mesopores of Silica-Based SBA-15 Materials Templated by Triblock Copolymers, *J. Am. Chem. Sci*. **2000**, *122*, 11925-11933.
7. A. Galarneau, H. Cambon, F. Di Renzo, F. Fajula, True Microporosity and Surface Area of Mesoporous SBA-15 Silicas as a Function of Synthesis Temperature, *Langmuir* **2001**, *17*, 8328-8335.
8. M. Kruk, M. Jaroniec, C. H. Ko, R. Ryoo, Characterization of the Porous Structure of SBA-15, *Chem. Mater*. **2000**, *12*, 1961-1968.
9. A. Silvestre-Albero, E. O. Jardim, E. Bruijn, V. Meynen, P. Cool, A. Sepulveda-Escribano, J. Silvestre-Albero, F. Rodriguez-Reinoso, Is There Any Microporosity in Ordered Mesoporous Silicas?, *Langmuir* **2009,** *25*, 939-943.
10. A. Galarneau, H. Cambon, F. Di Renzo, R. Ryoo, M. Choi, F. Fajula, Microporosity and connections between pores in SBA-15 mesostructured silicas as a function of the temperature of synthesis, *New J. Chem.* **2003**, *27*, 73-79.
11. S. A. Bagshaw, I. J. Bruce, Rapid calcination of high quality mesostructured MCM-41, MSU-X, and SBA-15 silicate materials: A step towards continuous processing?, *Microporous Mesoporous Mater*. **2008**, *109*, 199-209.
12. T. Benamor, L. Michelin, B. Lebeau, C. Marichal, Flash induction calcination: A powerful tool for total template removal and fine tuning of the hydrophobic/hydrophilic balance in SBA-15 type silica mesoporous materials, *Microporous Mesoporous Mater*. **2012**, *147*, 334-342.

13. F. Bérubé, S. Kaliaguine, Calcination and thermal degradation mechanisms of triblock copolymer template in SBA-15 materials, *Microporous Mesoporous Mater*. **2008**, *115*, 469-479.
14. J. P. Thielemann, F. Girgsdies, R. Schlögl, C. Hess, Pore Structure and Surface Area of Silica SBA-15: Influence of Washing and Scale-Up, *Beilstein J. Nanotechnol*. **2011**, *2*, 110-118.
15. R. van Grieken, G. Calleja, G. D. Dtucky, J. A. Melero, R. A. Garcia, J. Iglesias, Supercritical Fluid Extraction of a Nonionic Surfactant Template from SBA-15 Materials and Consequences on the Porous Structure, *Langmuir* **2003**, *19*, 3966-3973.
16. M. Barczak, Template removal from mesoporous silicas using different methods as tool for adjusting their properties, *New J. Chem.* **2018**, *42*, 4182-419.
17. B. Tian, X. Liu, C. Yu, F. Gao, Q. Luo, S. Xie, B. Tu, D. Zhao, Microwave assisted template removal of silicious porous materials, *Chem. Commun*. **2002**, 1186-1187.
18. L. Xiao, J. Li, H. Jin, R. Xu, Removal of organic templates from mesoporous SBA-15 at room temperature using UV/dilute H_2O_2, *Microporous Mesoporous Mater*. **2006**, *96*, 413-418.
19. L. M. Yang, Y. J. Wang, G. S. Luo, Y. Y. Dai, Simultaneous removal of copolymer template from SBA-15 in the crystallization process, *Microporous Mesoporous Mater*. **2005**, *81*, 107-114.
20. P. Pootawang, N. Saito, O. Takai, Solution Plasma Process for the template Removal in Mesoporous Silica Synthesis, *Jpn. J. Appl. Phys.* **2010**, *49*, 126202.
21. G. B. Alexander, W. M. Heston, R. K. Iler, The Solubility of Amorphous Silica in Water, *J. Phys. Chem.***1954**, *58*, 453-455.
22. M.-H. Yuan, L. Wang, R. T. Yang, Glow Discharge Plasma-Assisted Template Removal of SBA-15 at Ambient Temperature for High Surface Area, High Silanol Density, and Enhanced CO2 Adsorption Capacity, *Langmuir* **2014**, *30*, 8124-8130.
23. C.-M. Yang, B. Zibrowius, W. Schmidt, F. Schüth, Consecutive Generation of Mesopores and Micropores in SBA-15, *Chem. Mater*. **2003**, *15*, 3739-3741.
24. C.-M. Yang, B. Zibrowius, W. Schmidt, F. Schüth, Stepwise Removal of the Copolymer Template from Mesopores and Micropores in SBA-15, *Chem. Mater*. **2004**, *16*, 2918-2925.

25. Y. Liu, Z. Wang, C.-J. Liu, Mechanism of template removal for the synthesis of molecular sieves using dielectric barrier discharge, *Catal. Today*, **2015**, *256*, 137-141.
26. T. L. M. Maesen, H. W. Kouwenhoven, H. van Bekkum, B. Sulikowski, J. Klinowski, Template Removal from Molecular Sieves by Low-temperature Plasma Calcination, *Chem. Soc. Faraday Trans.* **1990**, *86*, 3967-3970.
27. Y. Liu, Y.-X. Pan, P. Kuai, C.-J. Liu, Template Removal from ZSM-5 Zeolite Using Dielectric-Barrier Discharge Plasma, *Catal. Lett.* **2010**, *135*, 241–245.
28. Y. Liu, Y. Pan, Z.-J. Wang, P. Kuai, C.-J. Liu, Facile and fast removal from mesoporous MCM-41 molecular sieve using dielectric-barrier discharge plasma, *Catal. Commun*. **2010**, *11*, 551-554.
29. L. Jia, A. Al Farouha, L. Pinard, S. Hedan, J.-D Comparot, A. Dufour, K. Ben Tayeb, H. Vezin and C. Batiot-Dupeyrat, New routes for complete regeneration of coked zeolite, *Appl. Catal. B: Env.* **2017**, *219*, 82-9.
30. L. Pinard, N. Ayoub, C. Batiot-Dupeyrat, Regeneration of a coked zeolite via non-thermal plasma process: a parametric study, *Plasma Chem. and Plasma Process.* **2019**, *39-4*,929-936.
31. A. Amir, C. Batiot-Dupeyrat, L. Pinard, Mechanism and Kinetic of Coke Oxidation by Non-thermal Plasma in Fixed Bed Dielectric Barrier Reactor, *J. Phys. Chem. C* **2019**, *123-14*, 9168-9175.
32. J. Landers, G. Yu. Gor, A. V. Neimark, Density functional theory method for characterization of porous materials, *Colloides and Surfaces A: Physiochem. Eng. Aspects* **2013**, *437*, 3-32.
33. S. Hudson, D. A. Tanner, W. Redington, E. Magner, K. Hodnett, S. Nakahara, Quantitative TEM analysis of a hexagonal mesoporous silicate structure, *Phys. Chem. Chem. Phys.* **2006**, *8*, 3467–3474.
34. S. Hitz, R. Prints, Influence of Template Extraction on Structure, Activity, and Stability of MCM-41 Catalysts, *J. Catal*. **1997**, *168*, 194-206.
35. B. Eliasson, U. Kogelschatz, Modeling and applications of silent discharge plasmas, *IEEE transactions on plasma science*, **1991**, *19*, 309-323.

36. B.M. Penetrante, M.C. Hsiao, J.N. Bardsley, B.T. Merritt, G.E. Vogtlin, A. Kuthi, C.P. Burkhart, J.R. Bayless, Identification of mechanisms for decomposition of air pollutants by non-thermal plasma processing, *Plasma Sources Sci. Technol*. **1997**, *6*, 251-259.
37. O. Legrini, E. Oliveros, A.M. Braun, Photochemical processes for water treatment, *Chem Rev.* **1993**, *93*, 671-698